Initial performance characterisation of a plasma thruster employing magnetic null regions

IEPC-2015-405／ISTS-2015-b-405

Presented at Joint Conference of 30th International Symposium on Space Technology and Science, 34th International Electric Propulsion Conference and 6th Nano-satellite Symposium
Hyogo-Kobe, Japan
July 4–10, 2015

Tom Wantock*, Charles Ryan†, Thomas Harle‡ and Aaron Knoll§
Surrey Space Centre, University of Surrey, Guildford, Surrey, GU2 7XH, United Kingdom

Abstract: The Halo thruster is a new cusped field thruster concept under development at the Surrey Space Centre, University of Surrey. The concept concerns the addition of magnetic null regions (defined as points of exact magnetic field cancellation enclosed by cusp structures) to a magnetic field topology closely resembling that of the Cylindrical Hall Thruster. Three variants of the concept have been developed: a proof-of-concept prototype using permanent magnets, centrally neutralised with a hollow cathode or a radio frequency electron source, and an electromagnetic prototype, neutralised with a downstream externally mounted hollow cathode. Measurements of thrust have been taken using pendulum thrust balances. Early results indicate performance comparable to other cusped field thrusters, with the electromagnetic Halo thruster delivering 21 mN thrust, 2200 s specific impulse, and 29% thrust efficiency with a 10 sccm Xenon anode flow rate at 767 W anode power.

Nomenclature

DC	= Direct Current
CHT	= Cylindrical Hall Thruster
EM	= Electromagnetic
η	= Thrust Efficiency
F	= Thrust
GIT	= Gridded Ion Thruster
HET	= Hall Effect Thruster
ID	= Inner Diameter
I_{sp}	= Specific Impulse
OD	= Outer Diameter
PM	= Permanently Magnetic
QCT	= Quad Confinement Thruster
RF	= Radio Frequency
SSC	= Surrey Space Centre

*PhD Student, Surrey Space Centre, Department of Electronic Engineering, t.wantock@surrey.ac.uk
†Research Assistant, Surrey Space Centre, Department of Electronic Engineering, c.ryan@surrey.ac.uk
‡Research Assistant, Surrey Space Centre, Department of Electronic Engineering, t.harle@surrey.ac.uk
§Lecturer in Electric Propulsion, Surrey Space Centre, Department of Electronic Engineering, a.knoll@surrey.ac.uk

I. Introduction

Through their efficient use of propellant mass in producing thrust, electric spacecraft propulsion technologies such as Gridded Ion Thrusters (GITs) and Hall Effect Thrusters (HETs) offer large potential savings in the cost of missions both near Earth and further afield.[1] These mature technologies have been successfully employed on commercial, military and scientific spacecraft which could accommodate their mass and power requirements, but integration with small satellites, with tight mass and power constraints, remains challenging. There exists a need for electric propulsion technologies which can operate efficiently at low powers and small sizes, as a result of increasing miniaturisation of spacecraft.[2]

The reductions in efficiency of conventional annular HETs in downscaling arise through effects such as increased surface to volume ratio, resulting in greater particle losses, and limitations in magnetic field strength, as a result of magnetic saturation of miniaturised magnetic circuits.[3] A significant motivation for the development of cusped field thrusters is to overcome these limitations through alternative magnetic field topologies. Plasma density tends to increase within cusp regions as a result of increased magnetic bottle confinement of electrons - it is thought that this could lead to improvements in thrust efficiency at small sizes and low powers, through increased ionisation and reduced particle losses to the thruster walls, while allowing high magnetic field strength through alternative magnetic field configurations.[4]

The Halo thruster, a technology currently under development at the Surrey Space Centre (SSC), University of Surrey, shares similarities with cusped field thrusters such as the Diverging Cusped Field Thruster,[5,6] the High Efficiency Multistage Plasma Thruster[7] and in particular the Cylindrical Hall Thruster (CHT).[4] The concept concerns points of exact magnetic field cancellation and associated cusp structures (referred to below as magnetic null regions) embedded within a magnetic field topology broadly resembling that of a CHT. In the following, the Halo thruster variants under development at the SSC are described and initial measurements of thrust, specific impulse and anode thrust efficiency are presented.

II. Halo Thruster Variants

Three variants of the Halo thruster, displayed in Figure 1, are currently under investigation at the SSC. A Halo thruster proof-of-concept prototype using permanent magnets (see Section III) has been tested in two of these variants: with a hollow cathode (designated DC-PM Halo for a DC discharge electron source with permanent magnets) and with an experimental radio frequency electron source (designated RF-PM Halo). A third variant uses electromagnets in place of permanent magnets and is neutralised by a hollow cathode (designated DC-EM Halo for a DC discharge electron source with electromagnets - see Section IV).

(a) DC-PM Halo Thruster (b) RF-PM Halo Thruster (c) DC-EM Halo Thruster

Figure 1: Halo thruster variants at the SSC.

III. DC-PM and RF-PM Halo Thrusters

A Halo thruster proof-of-concept prototype, displayed schematically in Figure 2a, uses permanent magnets to produce a magnetic field broadly similar to that of a CHT. This device acts as the plasma acceleration stage for the DC-PM and RF-PM Halo thruster variants. The device consists of concentrically arranged NdFeB annular magnets, housed around a boron nitride ceramic part (displayed in light grey) which also forms the walls of the discharge channel (of 46.5 mm OD, 23 mm length). The thruster's copper anode (displayed in red) sits at the outer edge of the discharge channel, while the cathode (not shown: a hollow cathode for the DC-PM variant, a radio frequency electron source for the RF-PM variant) is located on the central axis upstream of the thruster. Propellant is injected from the side of the device and flows around the anode to enter the discharge channel. A copper heat sink, with optional water cooling, is employed at the rear of the thruster, to mitigate against overheating of the magnets during extended operation. The dimensions of the assembled device, excluding the heat sink, are 72 mm OD and 44 mm length.

The magnetic field produced by this device differs in several respects from that of the CHT. Finite element simulation (using the free software Finite Element Method Magnetics, FEMM) reveals an annulus of exact magnetic field cancellation within the discharge channel, which is enclosed by a toroidal cusp structure. There also exists a point of exact magnetic field cancellation external to the discharge channel along the central axis, which is also enclosed by a cusp structure. These features (consisting of cancellation points enclosed by cusps) are collectively referred to as magnetic null regions - the internal toroidal magnetic null region is labelled the "halo", while the external point-like magnetic null region is labelled the "null point". Figure 2b displays the simulated magnetic field profile along the central axis, highlighted in red in Figure 2a, along the axial path intersecting the halo null region, highlighted in blue, and along an axial path from the top surface of the anode, highlighted in green. The halo null region is visible in the blue plot, while the downstream null point is visible in the red plot.

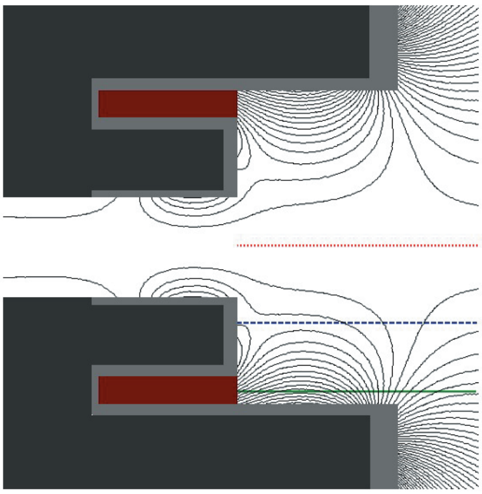

(a) Schematic and simulated magnetic field.

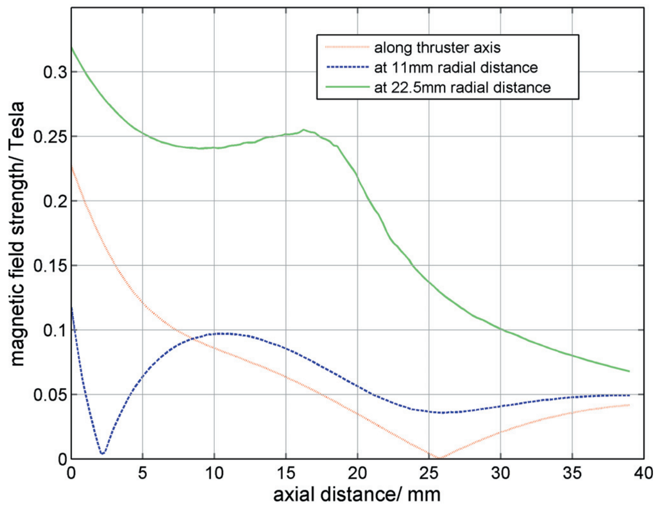

(b) Simulated total magnetic field strength profile along the central axis, along an axial path through the halo null region and along an axial path from the anode.

Figure 2: Halo thruster proof-of-concept, used in DC-PM and RF-PM Halo thruster variants.

The DC-PM Halo thruster variant combines the above prototype with a conventional hollow cathode built in-house, while the RF-PM Halo thruster variant makes use of an RF electron source, displayed in Figure 3. This device is derived from the nonambipolar electron source developed by Longmier et al.[8] It consists of a Pyrex source tube (of 55 mm ID, 60 mm OD, 170 mm length) with a 5 mm diameter exit orifice, within which an aluminium ion collection cylinder (of 48 mm ID, 54 mm OD, 90 mm length) is contained coaxially. Similarly to the nonambipolar electron source, eight equidistant axial slots of 60 mm length and 1 mm width are cut into the ion collection cylinder. Gas is fed into the device along the central axis through an aluminium plate fitted to the ion collection cylinder. Brass interface parts connect the RF electron source to the permanent magnet Halo thruster of Figure 2a. In contrast to the nonambipolar electron source, no magnetic field is applied and no grounded extraction ring at the orifice is employed - ions are lost to the grounded ion collection cylinder, allowing electrons to escape through the orifice to an external anode. The device has been measured to deliver up to 4 A to the thruster anode with fixed conditions of 200 W RF power and 4 sccm Krypton flow.

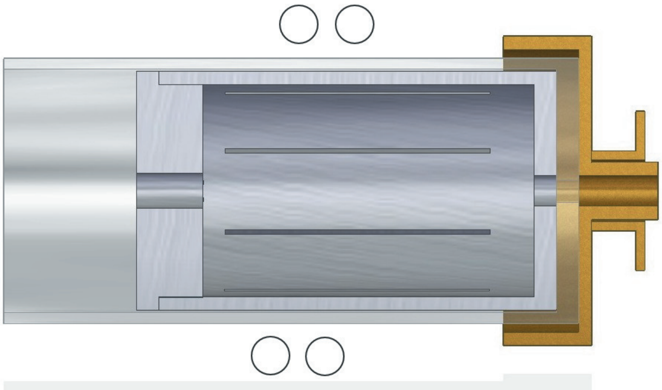

Figure 3: Schematic of RF electron source used in RF-PM Halo thruster.

IV. DC-EM Halo Thruster

The DC-EM Halo thruster is displayed schematically in Figure 4a. The thruster's magnetic field is produced by coaxial electromagnets and a magnetic circuit. The electromagnets are housed around a boron nitride ceramic part (displayed in light grey), which also forms the discharge channel (of 50 mm OD) - similarly to the CHT,[4] the channel is split into a coaxial section (of 20 mm ID, 14mm length) and a cylindrical section (of 35 mm length). The thruster's stainless steel anode (displayed in red) is situated in the coaxial part of the discharge channel, and contains holes in its top face through which propellant is fed. The hollow cathode neutraliser is mounted in the radial direction downstream of the channel exit, rather than upstream of the thruster on the central axis as is the case for the PM prototype. The overall dimensions of the assembled thruster are 150 mm OD and 74 mm length.

Finite element simulation of the magnetic field of this device reveals the presence of a halo null region internal to the thruster, and a downstream null point on the central axis. The magnetic field topology of this device differs from that of the proof-of-concept PM Halo thruster design in the separation of the halo null region and thruster anode by a strong radial magnetic field in the coaxial region - downstream of the halo, in the cylindrical region, the field topology is broadly similar to that of the PM thruster. Figure 4b displays simulated and experimentally measured radial magnetic field strength profiles for two axial paths from the inner and outer edges of the anode, and a simulated total magnetic field strength profile along the central axis, as highlighted in Figure 4a. The experimental measurements were made with an F. W. Bell 5170 Gauss-meter measuring the radial component of the magnetic field, attached to a 3-axis translation stage.

Along the outer channel wall (green path of Figure 4a) two peaks in magnetic field are observed, up to a maximum experimental value of 400 G. Good agreement between experiment and simulation is found. Between the two peaks of Figure 4b is a minimum that corresponds to the halo null region. Along the inner wall of the coaxial region (blue path of Figure 4a), the radial magnetic field peaks at almost 800 G, while the simulated total magnetic field along the central axis peaks at 900 G.

V. Experimental setup for thrust balance performance characterisation

Measurements of thrust performance of the three Halo thruster variants have been taken in the Electric Propulsion Laboratory of the SSC at the University of Surrey. The DC-PM and DC-EM Halo thruster experiments were conducted in the Daedalus vacuum chamber facility, a 2.5 m diameter by 3.5 m length chamber equipped with a turbomolecular pump and a cryogenic pump. This facility provides a typical base pressure of order 10^{-7} Torr and a typical background pressure of order 10^{-5} Torr during experiments.[9] The RF-PM Halo thruster experiment was conducted in the Pegasus vacuum chamber facility, a 2 m diameter by 1.5 m length chamber equipped with a turbomolecular pump. This facility provides a typical base pressure of order 10^{-6} Torr and a typical background pressure of order 10^{-5} Torr during experiments.[10]

Direct thrust measurements were completed using pendulum thrust balances. For the DC-PM Halo

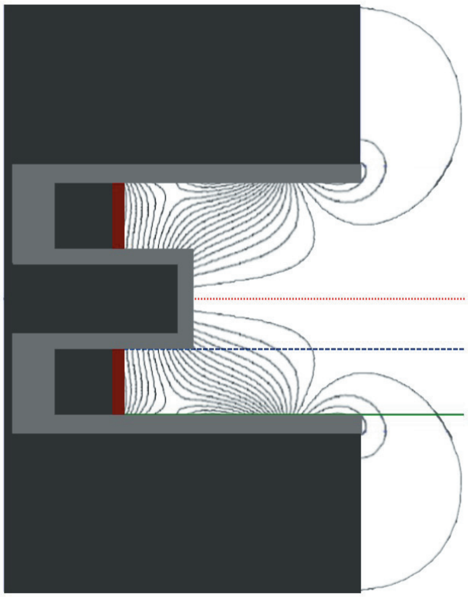

(a) Schematic and simulated magnetic field.

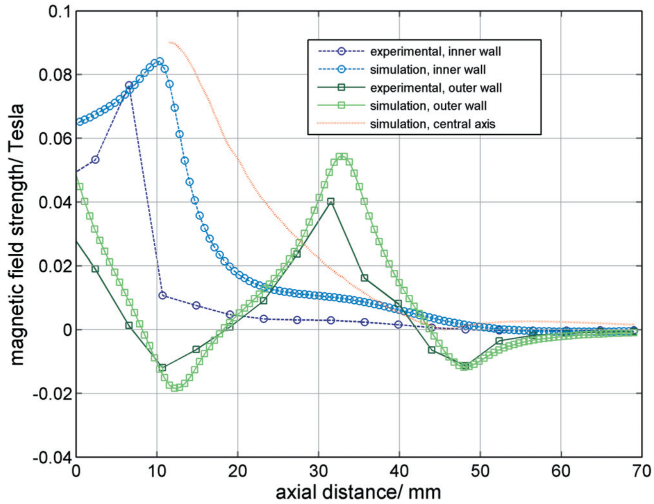

(b) Profiles of magnetic field strength along three axial paths, for 2 A current to electromagnets. The green and blue lines correspond to simulated and experimentally measured radial magnetic field strength, while the red line corresponds to simulated total magnetic field strength.

Figure 4: DC-EM Halo thruster.

thruster, thrust measurements were taken using an inverted pendulum thrust balance with a laser displacement sensor, previously developed at the SSC for experiments on the Quad Confinement Thruster (QCT), with a nominal sensitivity of 0.1 mN.[9] The RF-PM Halo thruster and DC-EM Halo thruster, as a result of their greater masses, were mounted to a hanging pendulum thrust balance previously developed for measurements of a high power QCT, also with a nominal sensitivity of 0.1 mN.[10]

Both thrust balances consist of a platform to which a thruster is mounted, which is free to move horizontally relative to a fixed structure. The platform is attached to the fixed structure by four aluminium flexures. In the case of the inverted pendulum balance the moving platform is situated above the fixed structure, while in the case of the hanging pendulum balance the moving platform hangs below the fixed structure. The horizontal displacement of the moving platform for each balance is measured using a Micro-Epsilon IDL1700-2 optical triangulation laser, with a resolution of 0.1 μm.[11] Each balance is calibrated by measuring the displacement of the moving platform as a result of an incrementally increased force applied by a stepper motor to a known mass, m, hanging from the moving platform. For a small horizontal displacement of the calibration mass, d, relative to the vertical distance between the mass and the platform, l, the force applied to the moving platform by the stepper motor is well approximated by mgd/l.

For the DC-PM and DC-EM Halo thruster experiments, which used a hollow cathode with a keeper current of 1.5 A, the cathode was not mounted to the thrust balance, in order to avoid excessive heating of the balance. For the RF-PM Halo thruster experiment, the components comprising the RF electron source were attached to the thrust balance, with the exception of the double loop antenna, which provided 200 W RF power. Measurements of thrust due to the RF electron source alone confirmed that thrust generated by the RF-PM Halo thruster is a result of the permanent magnet Halo acceleration stage.

In each experiment, the cathode was first initiated using a fixed flow rate and power setting before propellant was supplied to the anode. For the DC-PM and RF-PM Halo thruster variants, using permanent magnets, 300 V was applied to the anode to start the discharge in the presence of a magnetic field, while for the DC-EM Halo thruster, using electromagnets, a glow discharge was started before the magnetic field was subsequently applied. To take a measurement, each thruster was set to the desired power and anode flow rate conditions and operated continuously for 20 seconds, while data from the laser displacement sensor was acquired. The thruster was then turned off, and data continued to be acquired for another 20 second interval. Thrust was calculated from the difference between the average displacements of the balance before and after the thruster was turned off, taking into account the balance's calibration and measured thrust due to cold gas while the thruster was turned off. For the DC-EM Halo thruster, each measurement was repeated up to six times to give an average value, while for the DC-PM and RF-PM Halo thrusters one preliminary measurement was taken for each power and flow rate condition.

VI. Results

Figure 5 displays preliminary thrust measurement data as a function of anode power for the DC-PM and RF-PM Halo thruster variants, both of which used the PM proof-of-concept prototype displayed in Figure 2a. The DC-PM Halo thruster study focused on performance at low flow rates and low anode powers. The sensitivity of the thruster to various flow rate combinations was first mapped out at very low anode powers (10 to 20 W), before a power sweep, using a compromise of 2 sccm Krypton to both anode and cathode, was taken up to 100 W. The results of this early campaign demonstrated some potential for the concept - at 100 W anode power and very low flow rates of Krypton, the thruster delivered $F \sim 3$ mN, $I_{sp} \sim 1100$ s and $\eta \sim 10\%$. These results encouraged further investigation of the proof-of-concept prototype at higher powers and flow rates - this provided motivation for the RF-PM Halo thruster, in addition to motivation for the development of an RF electron source for use with a Hall effect discharge. Measurements of thrust were made at up to 600 W anode power, 15 sccm Krypton anode flow and 4 sccm Krypton cathode flow. The resulting data indicated that the PM prototype also operates favourably at higher flow rates and powers, with measured performance of $F \sim 10$ mN, $I_{sp} \sim 1600$ s and $\eta \sim 14$ % at 600W and 10 sccm Krypton anode flow rate. There is no plateau in performance apparent in the RF-PM Halo data, suggesting headroom for further improvement at higher powers. The discharge became unstable at powers beyond 300 W for the 7 sccm case. For each data point displayed in Figure 5, the nominal systematic uncertainty due to thrust balance resolution is of order 0.1 mN. Further experiments are required to characterise the proof-of-concept prototype beyond preliminary measurements. Establishing differences in behaviour of the DC-PM and RF-PM variants across identical flow rate and power conditions is a subject of on-going research.

Figure 6 displays DC-EM Halo thruster performance as a function of anode power, for two flow rates of Krypton and two settings of current supplied to the electromagnets. Measurements of thrust were taken up to around 800 W anode power at anode flow rates comparable to those used for the RF-PM Halo thruster experiment. The device delivered up to $F \sim 18$ mN, $I_{sp} \sim 2100$ s and $\eta \sim 23$ % over the conditions surveyed. The efficiency of the device appears to plateau around 300 W to 400 W: higher flow rates appear to push the plateau to higher powers. Higher magnetic field strength leads to higher efficiency at low powers, with the effect more pronounced at lower flow rates.

Figure 7 displays DC-EM Halo thruster performance for a 10 sccm Xenon flow rate and two settings of current supplied to the electromagnets, with Krypton data at identical volumetric flow and electromagnet current conditions included for comparison. With Xenon, the data collected suggest a level of performance for the device comparable to other cusped field thruster concepts, with $F \sim 21$ mN, $I_{sp} \sim 2200$ s and $\eta \sim 29$ % achieved at 767 W, with 2 A supplied to electromagnets. Performance is clearly enhanced as expected through the use of Xenon over Krypton. Further experiments are required to more thoroughly characterise the performance of the device using Xenon.

VII. Conclusion

The data presented in Figures 5-7 show measurements of performance taken during early stage development of the Halo thruster concept, which primarily concerns the addition of magnetic null regions (halo and null point) to a magnetic field topology broadly resembling that of the CHT. The concept is currently being explored through three thruster variants, using different combinations of permanent magnets/electromagnets and DC/RF electron sources. To date, the concept has shown some promise in the performance that can be delivered, with measured thrust values of the DC-EM Halo thruster exceeding 20 mN, specific impulse exceeding 2000 s, and efficiency approaching 30% for a 10 sccm Xenon anode flow rate, without extensive optimisation. More thrust measurements over a wider range of anode powers and flow rates are required to fully characterise the performance of each thruster variant.

In addition, it is essential that any deviation from the mechanism of the CHT due to the Halo thruster's modified magnetic field topology is established. This will be investigated through a series of plasma diagnostic experiments, starting with measurements of the PM proof-of-concept device, in order to guide future development. Key quantities to be measured include plasma density, plasma potential and electron temperature, using Langmuir and/or emissive probes and a 3-axis translation stage, and the ion energy distribution function in the exhaust plume, using a retarding field energy analyser.

Acknowledgments

The authors would like to thank Airbus Defence and Space, Airbus Group Innovations and Surrey Satellite Technology Ltd (SSTL) for funding and technical contributions to this research.

References

[1]D. M. Goebel and I. Katz, *Fundamentals of electric propulsion: ion and Hall thrusters*, vol. 1. John Wiley & Sons, 2008.

[2]J. Mueller, R. Hofer, and J. Ziemer, "Survey of propulsion technologies applicable to cubesats," *NASA JPL, Joint Army-Navy-NASA-Air Force (JANNAF), Colorado Springs, Colorado*, 2010.

[3]V. Zhurin, H. Kaufman, and R. Robinson, "Physics of closed drift thrusters," *Plasma Sources Science and Technology*, vol. 8, no. 1, p. R1, 1999.

[4]Y. Raitses and N. Fisch, "Parametric investigations of a nonconventional hall thruster," *Physics of Plasmas*, vol. 8, no. 5, pp. 2579–2586, 2001.

[5]D. Courtney and M. Martinez-Sanchez, "Diverging Cusped-Field Hall Thruster (DCHT)," *30th International Electric Propulsion Conference, Florence Italy*, 2007.

[6]C. Young, A. Smith, and M. Capelli, "Preliminary Characterization of a Diverging Cusped Field (DCF) Thruster," *31st International Electric Propulsion Conference, University of Michigan, Ann Arbor MI*, 2009.

[7]G. Kornfeld, N. Koch, and H. Harmann, "Physics and evolution of HEMP-Thrusters," *30th International Electric Propulsion Conference, Florence Italy*, 2007.

[8]B. Longmier, S. Baalrud, and N. Hershkowitz, "Nonambipolar electron source," *Review of scientific instruments*, vol. 77, no. 11, p. 113504, 2006.

[9]A. Knoll, D.Lamprou, V. Lappas, M. Pollard, and P. Bianco, "Thrust Balance Characterization of a 200 W Quad Confinement Thruster for High Thrust Regimes," *IEEE Transactions on Plasma Science*, vol. 43, no. 1, pp. 185–189, 2014.

[10]T. Harle, A. Knoll, V. Lappas, and P. Bianco, "Performance Measurements of a High Powered Quad Confinement Thruster," *33rd International Electric Propulsion Conference, George Washingston University, Washington D.C.*, 2013.

[11]S. Pottinger, D. Lamprou, A. Knoll, and V. Lappas, "Impact of plasma noise on a direct thrust measurement system," *Review of Scientific Instruments*, vol. 83, no. 3, p. 033504, 2012.

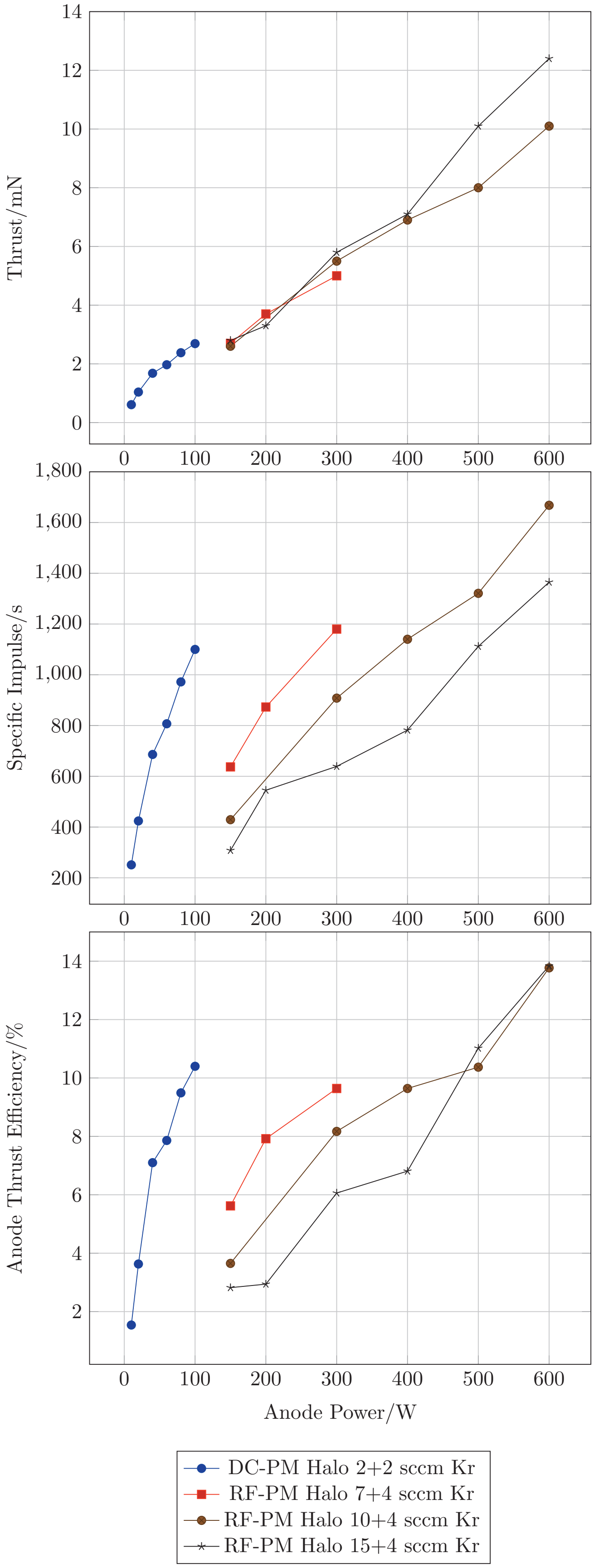

Figure 5: Preliminary results of thrust balance performance characterisation for the DC-PM and RF-PM Halo thruster variants, for several flow rates of Krypton. Flow rates are displayed in the format Anode Flow Rate + Cathode Flow Rate.

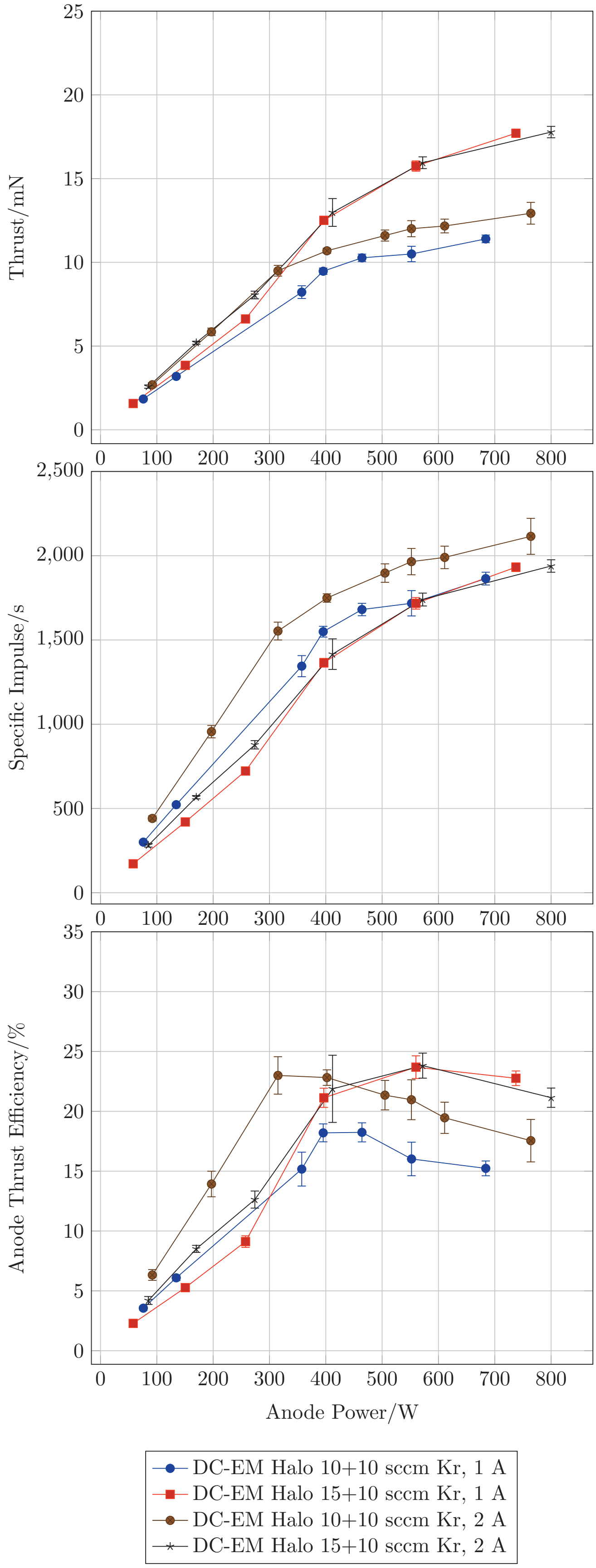

Figure 6: Results of thrust balance performance characterisation for DC-EM Halo thruster, for several flow rates of Krypton and for several currents applied to electromagnets. Flow rates are displayed in the format Anode Flow Rate + Cathode Flow Rate.

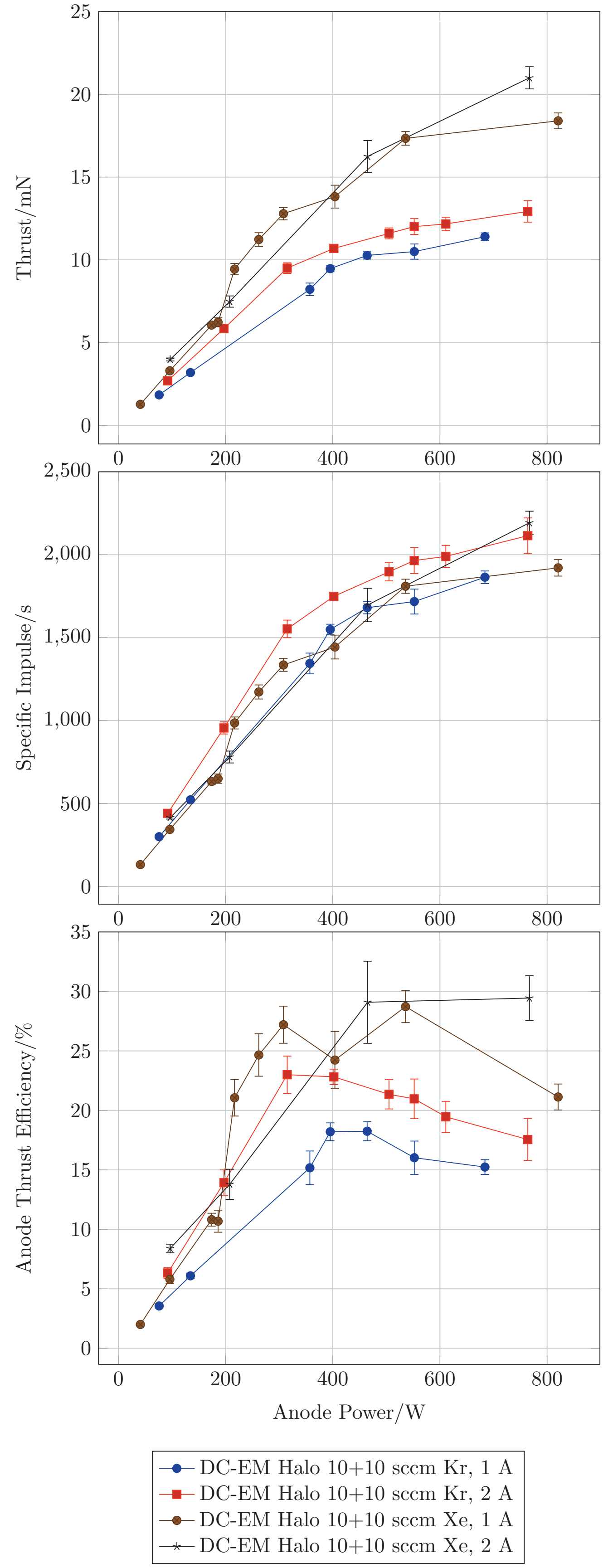

Figure 7: Results of thrust balance performance characterisation for DC-EM Halo thruster, comparing performance with Xenon to performance with Krypton, at identical volumetric flow rate conditions. Flow rates are displayed in the format Anode Flow Rate + Cathode Flow Rate.